

# Tracing Footsteps of Similar Cities: Modeling Urban Economic Vitality with Dynamic Inter-City Graph Embeddings

Xiaofeng Li<sup>\*\*</sup>, Xiangyi Xiao<sup>\*\*</sup>, Xiaocong Du<sup>\*</sup>, Ying Zhang<sup>\*</sup>, and Haipeng Zhang<sup>\*†</sup>

<sup>\*</sup>ShanghaiTech University, Shanghai, China

Email: lixf2022, xaoxy2025, duxc2023@shanghaitech.edu.cn,  
sgjzp.joyce@gmail.com, zhanghp@shanghaitech.edu.cn

**Abstract**—Urban economic vitality is a crucial indicator of a city’s long-term growth potential, comprising key metrics such as the annual number of new companies and the population employed. However, modeling urban economic vitality remains challenging. This study develops ECO-GROW, a multi-graph framework modeling China’s inter-city networks (2005-2021) to generate urban embeddings that model urban economic vitality. Traditional approaches relying on static city-level aggregates fail to capture a fundamental dynamic: the developmental trajectory of one city today may mirror that of its structurally similar counterparts tomorrow. ECO-GROW overcomes this limitation by integrating industrial linkages, POI similarities, migration similarities and temporal network evolution over 15 years. The framework combines a Dynamic Top-K GCN to adaptively select influential inter-city connections and an adaptive Graph Scorer mechanism to dynamically weight cross-regional impacts. Additionally, the model incorporates a link prediction task based on Barabasi Proximity, optimizing the graph representation. Experimental results demonstrate ECO-GROW’s superior accuracy in predicting *entrepreneurial activities and employment trends* compared to conventional models. By open-sourcing our code, we enable government agencies and public sector organizations to leverage big data analytics for evidence-based urban planning, economic policy formulation, and resource allocation decisions that benefit society at large.

**Index Terms**—region representation learning, graph neural networks, multi-graph learning, dynamic graphs

## I. INTRODUCTION

Urban economic vitality—reflecting a city’s overall economic health and growth potential [1]—is typically measured by two core indicators: the annual number of new companies and the population employed [2]. These factors, though distinct, are interconnected and serve as key measures of a city’s economic dynamics and growth potential [3]. Predicting these indicators remains challenging due to the complex, dynamic nature of urban economies. Existing approaches often rely on static, city-level aggregates, neglecting the evolving relationships between cities and their developmental trajectories [4]–[6]. However, cities are not isolated entities. The economic growth of one city can be influenced by and serve as a reference for structurally or geographically similar cities. For

instance, the Silicon Valley effect exemplifies how knowledge spillovers, fueled by research investment, skilled labor, and academic collaboration, lead to concentrated innovation in a specific region [7]. We also illustrate the changing inter-city relationships using Chongqing City as an example (Figure 1(a)). Cities with high industry similarity shifted from coastal regions in 2010 to larger northeastern cities in later years, reflecting the dynamic process of industrial convergence noted in prior studies on China’s economic development [8]. This observation highlights that modeling inter-city relationships together with their temporal evolution is essential for understanding and predicting urban economic vitality.

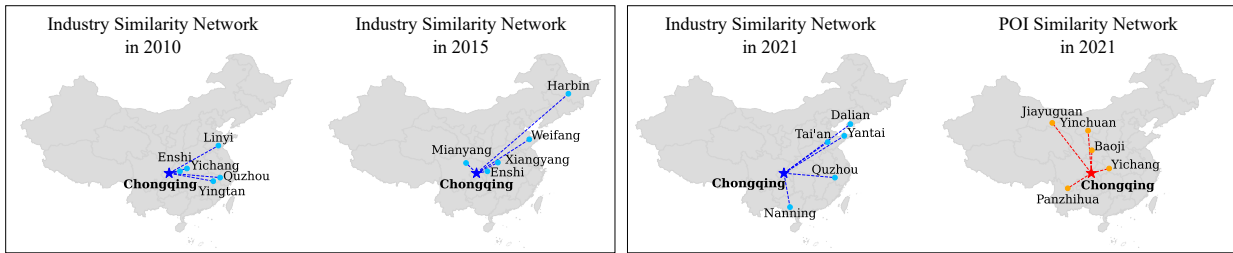
Traditional models often embed cities based only on local structures or attributes [4], [5], [9], overlooking broader inter-city economic linkages that drive parallel growth among cities. To address this limitation, we introduce a link prediction objective guided by Barabasi Proximity—a concept adapted from Barabasi’s product space theory [10]—to measure the likelihood of economic connections between cities based on industrial similarity. By leveraging domain-specific prior knowledge on industrial transfer patterns and economic dependencies, our framework learns embeddings that are more sensitive to inter-city economic relationships and better capture the structural dynamics of urban economies.

To comprehensively model urban economic vitality, it is essential to incorporate critical urban attributes. Beyond traditional statistical indicators [11], [12], and recent mobility networks [4]–[6], our framework introduces another two critical networks, regional economic connections and industrial structure [13], [14] (mentioned before in the Chongqing City case), which serves as a determinant and a consequence of economic growth [15].

We then focus on distinctive urban association representations under various attribute networks, as well as attribute fusion. As illustrated in Figure 1 (b), cities with high industry similarity can exhibit different POI similarity patterns, suggesting that different graphs capture heterogeneous structures. Therefore, to effectively utilize neighboring city information, our framework employs a Dynamic Top-K GCN (DTKGCN) module that dynamically adjusts the number of neighbors,

<sup>\*</sup> These authors contributed equally to this work.

<sup>†</sup> Corresponding author.



(a) Temporal Changes in Inter-City Similarity

(b) Comparison of Multi-Dimensional Inter-City Similarity

Fig. 1. The maps illustrate industry similarity dynamics and differences in city similarity networks, focusing on a part of China. The star marks Chongqing and the circles indicate the top five similar cities. (a) Shows changes in industry similarity over time. (b) Compares the top five similar cities across attributes.

$k$ , for each graph type. Unlike models that apply a fixed  $k$  value for all graphs [4], [6], the DTKGCN module allows the model to select the most relevant neighboring cities based on the unique characteristics of each graph (e.g., industry, POI, mobility networks). To further enhance the model’s ability to handle diverse networks, we introduce the Graph Scorer mechanism, which dynamically assigns weights to each static graph, ensuring that the most relevant graphs have a stronger influence on the final embedding.

Building on these insights, we propose **ECO-GROW** (Embedding of Cities through Optimized Graph Representation Of Weighted neighbors), a framework for modeling urban economic vitality through multi-graph learning. It integrates six inter-city networks to capture diverse urban attributes, employs a Dynamic Top-K GCN (DTKGCN) to adaptively select the most relevant neighbors for each network, and uses a Graph Scorer to balance their contributions. Guided by domain-specific prior knowledge from Barabasi’s complex network theory, ECO-GROW learns optimized graph representations that enable accurate prediction of new companies and employment trends, demonstrating strong practical value.

In summary, our contributions are summarized as follows:

- We propose a novel multi-graph framework ECO-GROW to model economic vitality representations, integrating dynamic inter-city information and static multi-network structures. By incorporating key modules like DTKGCN and Graph Scorer, our framework demonstrates superior performance in downstream tasks.
- We use domain-specific prior knowledge to supervise model training, enabling the model to better capture intricate economic relationships among cities. As a result, ECO-GROW outperforms all baselines, with significant improvements across all metrics, including a 20.46% reduction in RMSE and a 5.96% increase in  $R^2$ .
- This work demonstrates the robustness of ECO-GROW by testing on various downstream tasks and different time periods. The model shows the potential for other economic tasks, such as predicting housing market trends or income distribution, offering insights for policy making. We open-source the code<sup>1</sup> to foster research and applications in urban planning and policymaking.

<sup>1</sup>[https://github.com/sherry18510/ECO\\_GROW](https://github.com/sherry18510/ECO_GROW)

## II. RELATED WORK

### A. Graph Embedding

Graph embedding techniques represent graph structures in low-dimensional spaces, facilitating tasks like node classification and link prediction. Node2Vec [16] learns embeddings via biased random walks, preserving both local and global graph structures. Building on this, Graph Neural Networks (GNNs) leverage graph topologies and node features. The Graph Convolutional Network (GCN) [17] aggregates information from local neighborhoods, while the Graph Attention Network (GAT) [18] uses attention mechanisms to weigh neighbors’ importance. Graph Autoencoder (GAE) [9] takes an unsupervised approach by reconstructing graph topology to capture latent representations. The advances in graph embedding offer powerful and insightful tools to enhance traditional region embedding approaches.

### B. Region Representation Learning

Region representation learning focuses on modeling relationships between urban attributes, which are traditionally applied to tasks such as crime rate prediction, check-in frequency analysis, and land-use classification. Recent advancements have shifted toward integrating diverse properties through more sophisticated methods [19]–[22]. For example, MVURE [4] employs a multi-view learning framework with adaptive weight assignment to fuse human mobility and region attributes, demonstrating strong performance in tasks like crime prediction. Similarly, MGFN [5] utilizes a multi-graph fusion module and cross-attention mechanisms to capture relationships within mobility graphs. HREP [6] constructs a heterogeneous region graph by integrating human mobility, geographic proximity, and POI distributions while leveraging self-attention and prompt learning to align embeddings with downstream tasks. Inspired by these approaches, our work extends region representation learning to model spatiotemporal dynamics for urban economic forecasting, addressing the unique challenges of predicting entrepreneurial growth.

## III. PRELIMINARIES

### A. Multi-Graph Construction

Cities are complex systems characterized by geographic, mobility, and industrial attributes. To model these relationships, we construct six networks  $\mathcal{G} = \{G_{\text{dist}}, G_s, G_d, G_{\text{poi}}, G_{\text{ind}}, G_{\text{emp}}\}$ , each capturing a specific attribute.

1) *Distance Network*  $G_{dist}$ : constructed using the inverse of geographic distance between cities to reflect spatial closeness.

2) *Population Flow Network*  $G_s, G_d$ : built from migration data, where similarity is measured by the cosine similarity of source and destination distributions [4].

3) *POI Similarity Network*  $G_{poi}$ : derived from the TF-IDF representations of POI categories in each city to capture similarity.

4) *Industry Similarity Network*  $G_{ind}$ : constructed in a similar way, comparing cities' industrial compositions using TF-IDF and cosine similarity.

5) *Original Feature Clustering Network*  $G_{emp}$ : generated by clustering cities based on explicit socioeconomic features (e.g., GDP, population) using K-means.

## B. Problem Statement

Given the city characteristics  $F$  and the set of correlation networks  $\mathcal{G}$ , the goal of modeling urban economic vitality is to learn a distributed and low dimensional embedding of each city, which is denoted as  $\mathcal{E}^t$ ,

$$\mathcal{E}^t = \{e_1^t, e_2^t, \dots, e_n^t\}, \quad e_i^t \in \mathbb{R}^d, \forall i \in [1, n]$$

where  $e_i^t$  denotes the embedding of city  $i$  in year  $t$ , and  $d$  is the dimension of embedding.

## IV. METHODOLOGY

This section introduces the proposed model ECO-GROW, with its overall framework shown in Figure 2(a). In the following sections, we will elaborate (1) DTKGCN, (2) Graph Scorer, (3) learning objectives, and (4) the overall process pipeline of the proposed ECO-GROW.

### A. DTKGCN

In the field of Graph Neural Networks (GNNs), effective aggregation of information from neighboring nodes is fundamental to model performance. Traditional GCNs utilize uniform aggregation, which can dilute crucial information due to noise or sparsity [23]. Furthermore, many models rely on fixed neighborhood sizes, which may not capture the most relevant information, especially in dynamic graphs with heterogeneous structures. To enhance this aggregation process, we introduce a mechanism called Dynamic Top-K GCN (DTKGCN), which adaptively selects the top-k most relevant neighbors based on the characteristics of each graph type, as shown in Figure 2(b).

The DTKGCN layer takes a node feature matrix  $X \in \mathbb{R}^{N \times F_{in}}$  and an adjacency matrix  $A \in \mathbb{R}^{N \times N}$ , where  $N$  represents the number of nodes and  $F_{in}$  denotes the input feature dimension. The output is a new representation  $H_{agg} \in \mathbb{R}^{N \times F_{out}}$ , where  $F_{out}$  is the output feature dimension.

Initially, the node features undergo a linear transformation:

$$H = XW \in \mathbb{R}^{N \times F_{out}} \quad (1)$$

where  $W \in \mathbb{R}^{F_{in} \times F_{out}}$  is the weight matrix, and  $H$  represents the transformed node features.

After this transformation, we move on to the neighbor aggregation process. For each graph

$g \in \{G_{dist}, G_{poi}, G_s, G_d, G_{ind}\}$ , we introduce  $k_g$ , a learnable parameter that determines the number of top neighbors to consider during the aggregation process. This parameter is optimized during the training process via gradient descent, where  $k_g$  is treated as a continuous parameter during backpropagation but discretized during forward aggregation. Next, we compute edge weights from the adjacency matrix to identify the top  $k_g$  neighbors for each node in graph  $g$ . For a given node  $i$  in graph  $g$ , the following operation is performed:

$$\mathcal{I}_{top-k_g} = \text{top-}k_g(A_g[i], k_g) \quad (2)$$

The top- $k_g$  function returns indices of the top  $k_g$  neighbors based on their edge weights in  $A_g[i]$ .

The aggregation of features is conducted solely from the selected top  $k_g$  neighbors. The aggregation process for each node  $i$  is defined as follows:

$$H_{agg}[i] = \max_{j \in \mathcal{I}_{top-k_g}[i]} H[j] \quad (3)$$

By taking the maximum value from the features of the top  $k_g$  neighboring nodes, the new feature representation for node  $i$  is derived as  $H_{agg}[i]$ .

### B. Graph Scorer

In multi-graph tasks, balancing multiple network structures is a critical challenge, as each network may contribute differently to the final representation. To address this, we propose the Graph Scorer module, which automatically learns the weight of each graph, enabling adaptive feature aggregation that reflects the varying importance of different networks.

Formally, let  $\mathbf{Z}_g$  denote the static graph features for each graph  $g \in \{G_{dist}, G_{poi}, G_s, G_d, G_{ind}, G_{emp}\}$ . The Graph Scorer assigns each graph a softmax-normalized importance weight  $w_g$ , defined as:

$$w_g = \frac{\exp(s_g)}{\sum_{g' \in \mathcal{G}} \exp(s_{g'})} \quad (4)$$

where  $s_g$  is a learnable scalar parameter of the graph  $g$ . These weights  $w_g$  are dynamically updated during training to reflect the contribution of each graph to the overall learning process. The weighted feature representation  $\mathbf{Z}_{static}^t$  is computed as the weighted sum of the individual graph features:

$$\mathbf{Z}_{static}^t = \sum_{g \in \mathcal{G}} w_g \cdot \mathbf{Z}_g^t \quad (5)$$

where  $\mathbf{Z}_{static}^t$  is the aggregated representation that integrates information from all static graphs.

### C. Learning Objectives

To ensure the learned embeddings effectively capture implicit economic relationships and dynamic changes, we design a supervised learning framework guided by complex prior knowledge. Specifically, we utilize the Barabasi Proximity, a well-established theory in complex networks, to distill meaningful information into the embeddings. The training process adopts a multi-task learning approach with two objectives:

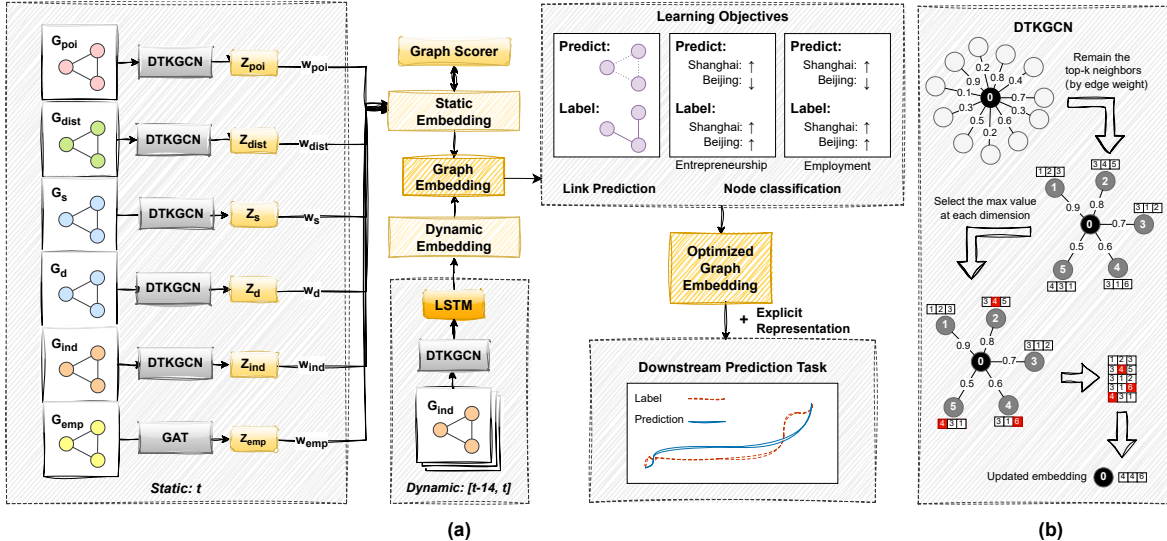


Fig. 2. (a) The overall architecture of ECO-GROW. (b) DTKGCN Module: For each node in a certain graph  $g$ , the top- $k_g$  neighbors are selected, retaining the maximum value in each dimension to form the new embedding.

node classification to model individual city growth patterns and link prediction to incorporate inter-city industrial proximity. Joint optimization enables the model to encode both local city characteristics and inter-city economic dependencies.

*1) Node Classification of Economic Growth Rate:* The node classification task focuses on predicting the direction of economic change for each city, encompassing two key indicators: the growth rate of new companies and population employed. Specifically, it aims to determine whether the two indicators in a city from the previous year to the current year are positive or negative. We define the growth rate for both new companies and employed population first. The growth rate of new companies in city  $i$  from year  $t-1$  to year  $t$  is given by:

$$r_{\text{comp}} = \frac{y_{\text{comp}}^t - y_{\text{comp}}^{t-1}}{y_{\text{comp}}^{t-1}} \quad (6)$$

where  $y_{\text{comp}}^t$  represents the number of new companies in city  $i$  in year  $t$ , and  $y_{\text{comp}}^{t-1}$  represents the previous year. Similarly, the growth rate of employed population  $r_{\text{emp}}$  can be calculated in the same way.

This task is crucial for capturing the temporal volatility of urban economic growth, as reflected in prior studies on dynamic economic systems [24]. The Binary Cross-Entropy Loss (BCELoss) for this task is:

$$\mathcal{L}_{\text{NC}} = \alpha \cdot \text{BCELoss}(r_{\text{comp},\text{true}}, r_{\text{comp},\text{pred}}) + (1 - \alpha) \cdot \text{BCELoss}(r_{\text{emp},\text{true}}, r_{\text{emp},\text{pred}}) \quad (7)$$

where  $r_{\text{true}}$  and  $r_{\text{pred}}$  represent the ground truth and predicted labels, respectively.

*2) Link Prediction in Barabasi Network:* To incorporate complex economic relationships between cities, we define a link prediction task based on the Barabasi Proximity [10], which captures industrial transfer patterns and economic dependencies. This inter-city proximity measurement involves three main stages: a) revealed comparative advantage (RCA) calculation b) proximity matrix construction c) algorithm implementation.

*a) Revealed Comparative Advantage (RCA) Calculation:* For each city  $c$  and industry  $i$ , we calculate the Revealed Comparative Advantage (RCA) as:

$$RCA_{c,i} = \frac{\frac{E_{c,i}}{\sum_i E_{c,i}}}{\frac{\sum_c E_{c,i}}{\sum_{c,i} E_{c,i}}} \quad (8)$$

where  $E_{c,i}$  represents the number of new firm registrations in industry  $i$  located in city  $c$ . Cities with  $RCA_{c,i} \geq 1$  are considered to have a comparative advantage in industry  $i$ .

*b) Proximity Matrix Construction:* The proximity  $\phi_{c,c'}$  between two cities  $c$  and  $c'$  is calculated using conditional probability:

$$\phi_{c,c'} = \min(P(c'|c), P(c|c')) \quad (9)$$

where  $P(c'|c)$  represents the probability that city  $c'$  has RCA in an industry where city  $c$  also has RCA. This symmetric measure ensures robustness to extreme values.

*c) Algorithm Implementation:* The calculation process is implemented through the following key steps:

#### Algorithm 1 Inter-City Proximity Calculation

- 1: Initialize temporal range  $[t_{\text{start}}, t_{\text{end}}]$
- 2: Filter registrations data within specified time window
- 3: Extract unique city list  $\mathbf{C}$  and industry list  $\mathbf{I}$
- 4: Compute RCA matrix  $\mathbf{R} \in \mathbb{R}^{|\mathbf{C}| \times |\mathbf{I}|}$
- 5: Binarize RCA matrix  $\mathbf{B}$  where  $B_{c,i} = \mathbb{I}(RCA_{c,i} \geq 1)$
- 6: Initialize proximity matrix  $\Phi \in \mathbb{R}^{|\mathbf{C}| \times |\mathbf{C}|}$
- 7: **for** each city pair  $(c_i, c_j) \in \mathbf{C} \times \mathbf{C}$  **do**
- 8:     Compute co-occurrence:  $N_{ij} = \sum_k B_{i,k} \cdot B_{j,k}$
- 9:     Compute conditional probabilities:
- 10:      $P(c_j|c_i) = \frac{N_{ij}}{\sum_k B_{i,k}}$
- 11:      $P(c_i|c_j) = \frac{N_{ij}}{\sum_k B_{j,k}}$
- 12:      $\Phi[i,j] \leftarrow \min(P(c_j|c_i), P(c_i|c_j))$
- 13: **end for**
- 14: Construct Maximum Spanning Tree (MST) from  $\Phi$
- 15: Remain the edges with  $\Phi \geq \Phi'$

The Maximum Spanning Tree construction guarantees that all cities remain connected through their most significant industrial relationships, while the threshold filtering removes weak connections that may introduce noise to the link prediction task. Through this construction process, we obtain a binary adjacency matrix where each entry indicates whether two cities share significant industrial proximity (presence or absence of an edge).

This task directly supervises the embeddings to reflect inter-city industrial dynamic space as a key aspect of the economic landscape. The BCELoss for this task is denoted as:

$$\mathcal{L}_{LP} = \text{BCELoss}(e_{\text{true}}, e_{\text{pred}}) \quad (10)$$

where  $e_{\text{true}}$  and  $e_{\text{pred}}$  represent the ground truth and predicted edge weights, respectively.

3) *Combined Learning Objective*: To balance the contributions of the node classification and link prediction tasks, we introduce a weighted loss function:

$$\mathcal{L} = \lambda \cdot \mathcal{L}_{NC} + (1 - \lambda) \cdot \mathcal{L}_{LP} \quad (11)$$

where  $\lambda$  is a hyperparameter that controls the relative importance of each task.

#### D. Model Pipeline

The proposed model, ECO-GROW, as illustrated in Figure 2(a), is designed to predict city-level economic vitality by learning distributed embeddings that capture both static and dynamic characteristics of cities. The model takes as input a static graph of the year  $t$  and a series of dynamic graphs representing the past 15 years. After training, ECO-GROW generates implicit city-level representations for each year as a basis for downstream tasks.

For the static graphs, ECO-GROW utilizes six static networks. DTKGCN is applied to  $G_{\text{dist}}^t$ ,  $G_{\text{POI}}^t$ ,  $G_S^t$ ,  $G_D^t$ , and  $G_{\text{ind}}^t$  to capture multi-dimensional similarities by aggregating information from the most relevant neighbors. For  $G_{\text{emp}}^t$ , a GAT layer [18] is used to automatically learn city relationships without predefining correlations. This process results in an embedding  $Z_g^t$  for each static graph. To aggregate these embeddings, ECO-GROW uses a weighted combination learned through a Graph Scorer, forming the final static representation  $Z_{\text{static}}^t$ .

For dynamic graphs, ECO-GROW focuses on the temporal evolution of the industry network  $\{G_{\text{ind}}^{t-14}, \dots, G_{\text{ind}}^t\}$  over the past 15 years. Each graph in the sequence is processed by a DTKGCN layer to extract time-step features  $Z_{\text{dyn}}^\tau$ , where  $\tau \in [t-14, t]$ . These temporal features are then passed through LSTM [25] to model historical dependencies and produce dynamic representations:

$$\mathbf{H}_{\text{dyn}}^t = \text{LSTM}([Z_{\text{dyn}}^{t-14}, \dots, Z_{\text{dyn}}^t]) \quad (12)$$

The static representation  $Z_{\text{static}}^t$  and the dynamic representation  $\mathbf{H}_{\text{dyn}}^t$  are concatenated with explicit node-level features  $F^t$  to form a unified embedding for all cities at  $t$ :

$$\mathcal{E}^t = \text{ReLU}([Z_{\text{static}}^t, \mathbf{H}_{\text{dyn}}^t, F^t]) \quad (13)$$

ECO-GROW optimizes the joint learning objective of node classification and link prediction. Once training converges, the model retains the learned embeddings  $\mathcal{E}^t$  as an implicit representation of city-level economic growth.

## V. EXPERIMENTS

To evaluate the effectiveness of the learned economic growth embeddings in year  $t$ , we conduct two downstream regression tasks: one using the number of new companies in year  $t+1$  as the target label, and the other using employment population in year  $t+1$  as the target label. The embedding for each city in year  $t$  is concatenated with explicit city features (e.g., GDP, population) to form a combined representation, which is fed into two separate regression models to do predictions. We calculate all metrics to ensure robust and generalized evaluations of our model's performance. The experiments intend to answer the following questions:

- **RQ1:** Does our framework (ECO-GROW) improve the performance and robustness compared to the baseline models?
- **RQ2:** Is each component of the model effective to ECO-GROW?
- **RQ3:** Is ECO-GROW sensitive to the hyperparameters of different components?

#### A. Experiment Settings

1) *Data Description*: We collect four real-world datasets, which focus on 297 cities across China. (1) **City Features**<sup>2</sup>: This city-level information includes economic indicators like GDP, population, and employment, from the year 2005 to 2022. (2) **Entrepreneurship data**: This dataset includes information about the registration of startups across time, cities, and industries, from the year 2005 to 2022. (3) **POI data**<sup>3</sup>: This dataset provides location-based information about Points of Interest in Chinese cities, from the year 2019 to 2021. (4) **Mobility data**<sup>4</sup>: This dataset includes information about population movement between Chinese cities, from the year 2019 to 2021.

These datasets are utilized as explicit representations, information for computing edge weights, and ground truth labels in our framework. Specifically, for the two prediction tasks, we focus on the Entrepreneurship data and the employment data from the Explicit Features dataset. To ensure consistency across datasets, we align the data for each city and year in the four datasets.

2) *Implementation Details*: Our proposed model is implemented using PyTorch and PyTorch Geometric. All experiments are conducted on a server equipped with Intel Xeon Gold 5218 CPU @ 2.30GHz (128 cores), 1TB RAM, and NVIDIA RTX 3090 24GB GPU. After parameter tuning, the embedding size of each city is set to  $d = 16$ , and the parameters that control the loss value of the learning objectives are set to  $\alpha = 0.6$  and  $\lambda = 0.5$  respectively. We use a learning rate of

<sup>2</sup><https://www.stats.gov.cn/english>

<sup>3</sup><https://lbsyun.baidu.com>

<sup>4</sup><https://report.amap.com/migrate/page.do>

0.01 and train each baseline model for 250 epochs. We use grid search to determine the optimal value of the L1 normalization weight in the Lasso regression model [26], within the range of  $\{1 \times 10^{-3}, 1 \times 10^{-4}, 1 \times 10^{-5}, 1 \times 10^{-6}\}$ . We calculate all metrics using a K-Fold cross-validation approach with  $K = 5$ , ensuring robust and generalized evaluations of our model’s performance.

3) *Baseline Algorithms*: We conduct experiments on the following baseline models, categorized into two types according to whether they rely on explicit or implicit representations. All baseline models are designed with the objective of generating city embeddings, enabling a fair comparison with our model.

(1) Explicit baselines: These methods directly use observable city attributes. Yet they do not capture hidden, complex relationships across multiple city attributes.

- **Explicit Features**: Uses raw indicators (e.g., GDP, population, new companies, employment in year t) as input to a Lasso regression.
- **Moving Window**: Captures temporal dynamics by using new companies and population employed over the past 15 time steps as sequential features.

(2) Implicit baselines: These methods aim to learn latent city embeddings using graph-based or region embedding techniques. Yet they fail to capture the dynamic nature of urban systems and the broader inter-city economic relationships.

- **Node2Vec** [16]: Learns node embeddings by performing biased random walks on the graph.
- **Graph Autoencoder (GAE)** [9]: Encodes city graphs into latent embeddings by reconstructing graph topology.
- **MVURE** [4], **MGFN** [5], **HREP** [6]: Multi-graph or heterogeneous region embedding frameworks that fuse multiple urban networks through attention or adaptive weighting. HREP represents the current state-of-the-art in multi-graph region embedding.

For explicit baselines, we use features directly as input for downstream tasks. For implicit baselines, we apply recommended hyperparameters, input static networks from year  $t$ , and build task-specific objectives. Each model is trained for 250 epochs to produce a 16-dimensional embedding, which is then combined with explicit features for evaluation.

### B. Result Analysis (*RQ1*)

Table I and II list the performance of all models in 2019, 2020, and 2021, as well as their average results for predicting the number of new companies and the employment population respectively. It is important to note that the result for  $t$  means that we use the data from before and  $t$  to predict the number of new companies in year  $t + 1$ .

1) *Performance Across Tasks*: For both prediction tasks, new companies and employment population, ECO-GROW consistently outperforms all baselines in RMSE, MAE, and  $R^2$ . Specifically, ECO-GROW reduces RMSE and MAE by 20.46% and 18.81% respectively, and improves  $R^2$  by 5.96% in the first task.

Although Explicit Features achieves the second-best performance for entrepreneurship and MGFN ranks second for employment, their improvements are limited due to their reliance on static attributes or single-view supervision. The moving window method has inherent limitations in capturing long-term trends and dynamic changes in economic systems. Node2Vec and GAE, on the other hand, rely heavily on fixed neighborhood structures and static graph representations. In contrast, ECO-GROW utilizes complex prior knowledge alongside dynamic information to better model temporal trends in economic growth.

2) *Robustness Across Tasks*: While some baselines perform well on individual tasks, they lack consistency across both. ECO-GROW maintains stable superiority in all evaluations, demonstrating strong generalization. To better understand the complexity and stability of the two downstream tasks, we calculate the KL divergence between yearly distributions: smaller values indicate greater stability and simplicity.

As shown in Figure 3, entrepreneurship prediction exhibits a higher KL divergence compared to the employment prediction in all years, suggesting that the former task is more challenging than the latter. ECO-GROW shows solid improvements in both tasks, with a more substantial enhancement in the challenging one, demonstrating its superior capability to handle more complex urban economic indicators.

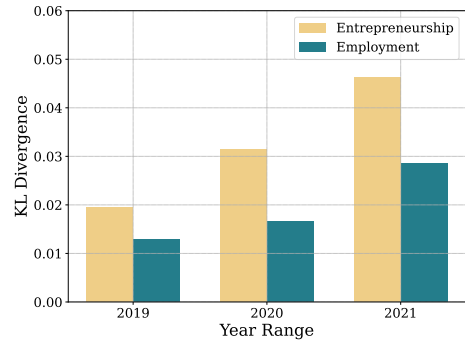


Fig. 3. KL Divergence between years for two downstream tasks. For year  $t$ , the result represents the distribution shift for each task from the previous year  $t - 1$  to the current year  $t$ .

3) *Robustness Across Years*: Although HREP and MVURE perform well in the year 2021 and year 2020 respectively, ECO-GROW consistently outperforms all baseline models in both tasks across all three years (2019, 2020, and 2021), demonstrating its ability to maintain strong performance over time. This stable performance further underscores the robustness of ECO-GROW, showing that it is not sensitive to annual variations in the data and can be relied upon for forecasting across different periods.

### C. Ablation Analysis (*RQ2*)

We conduct three ablation experiments focusing on both downstream tasks and the results are shown in Tabel III and Table IV respectively. For the entrepreneurship prediction task, replacing the DTKGCN layer with a standard GCN (w/o DTKGCN) increases RMSE by 18.14% on average. Removing

TABLE I

PREDICTION ERRORS AND GOODNESS OF FIT FOR FORECASTING THE NUMBER OF NEW COMPANIES ACROSS CHINESE CITIES. RESULTS FOR YEAR  $t$  USE DATA UP TO  $t$  TO PREDICT COMPANIES IN  $t + 1$ . THE BEST RESULT IS IN **BOLD** AND THE RUNNER-UP IS UNDERLINED.

Metric	Year	Explicit Features	Moving Window	node2vec	GAE	HREP	MVURE	MGFN	ECO-GROW
RMSE $\downarrow$	2019	<u>16726.499</u>	23619.512	21843.818	22107.894	19328.523	18787.233	17165.253	<b>16029.035</b>
	2020	<u>21012.320</u>	30559.153	22812.730	22510.601	22636.571	<u>20301.098</u>	20978.207	<b>15303.907</b>
	2021	23924.155	28231.584	24909.030	30433.218	<u>23576.446</u>	<u>26243.253</u>	23869.707	<b>17710.724</b>
	Average	<u>20554.324</u>	27470.083	23188.526	25017.238	21847.180	21777.195	20671.056	<b>16347.888</b>
MAE $\downarrow$	2019	8500.289	11628.066	11954.124	10766.108	11067.699	10592.544	<u>8370.484</u>	<b>8199.070</b>
	2020	<u>11490.189</u>	15397.325	12919.301	13920.786	13889.582	11678.060	12029.129	<b>9439.828</b>
	2021	16923.181	19163.416	17698.153	18496.387	<u>16355.492</u>	18038.560	16933.148	<b>12332.495</b>
	Average	<u>12304.553</u>	15396.269	14190.526	14394.427	13770.924	13436.401	12444.254	<b>9990.464</b>
$R^2\uparrow$	2019	<u>0.851</u>	0.682	0.441	0.776	0.838	0.817	0.824	<b>0.855</b>
	2020	0.849	0.670	0.811	0.828	0.817	<u>0.861</u>	0.844	<b>0.909</b>
	2021	0.817	0.763	0.801	0.728	<u>0.826</u>	0.785	0.819	<b>0.905</b>
	Average	<u>0.839</u>	0.705	0.684	0.778	<u>0.827</u>	0.821	0.829	<b>0.889</b>

TABLE II

PREDICTION ERRORS AND GOODNESS OF FIT FOR FORECASTING POPULATION EMPLOYED ACROSS CHINESE CITIES. RESULTS FOR YEAR  $t$  USE DATA UP TO  $t$  TO PREDICT COMPANIES IN  $t + 1$ .

Metric	Year	Explicit Features	Moving Window	node2vec	GAE	HREP	MVURE	MGFN	ECO-GROW
RMSE $\downarrow$	2019	12.375	17.310	12.217	11.920	12.476	11.615	<u>11.030</u>	<b>11.025</b>
	2020	16.850	20.274	14.851	14.933	17.073	15.882	<u>14.414</u>	<b>13.968</b>
	2021	<u>15.016</u>	17.560	17.245	16.205	16.514	15.360	16.039	<b>14.196</b>
	Average	14.747	18.381	14.771	14.353	15.355	14.286	<u>13.827</u>	<b>13.063</b>
MAE $\downarrow$	2019	6.418	6.950	6.053	5.679	7.327	4.913	<u>4.652</u>	<b>4.589</b>
	2020	6.552	7.274	6.134	6.064	8.577	6.534	<u>5.447</u>	<b>5.368</b>
	2021	8.463	<u>7.445</u>	8.155	8.457	8.516	7.540	7.705	<b>6.858</b>
	Average	7.144	7.223	6.781	6.733	8.140	6.329	<u>5.935</u>	<b>5.605</b>
$R^2\uparrow$	2019	0.950	0.944	0.941	0.954	0.955	0.962	<u>0.964</u>	<b>0.965</b>
	2020	0.921	0.901	0.925	0.927	0.910	0.927	<u>0.935</u>	<b>0.937</b>
	2021	0.935	0.933	0.888	0.927	0.922	<u>0.936</u>	0.931	<b>0.944</b>
	Average	0.935	0.928	0.918	0.936	0.929	0.942	<u>0.944</u>	<b>0.949</b>

the Graph Scorer (w/o GS) and directly concatenating graph features raises  $R^2$  by 6.52%, underscoring the importance of learning graph weights. Eliminating the dynamic graph input and LSTM module (w/o LSTM) leads to a 9.99% MAE increase, demonstrating their necessity for capturing temporal dynamics. Similarly, for employment trends prediction, the ablation experiments demonstrate a similar pattern of results. The full model consistently surpasses ablated versions across all metrics, confirming the effectiveness of its key components.

TABLE IV  
ABLATION RESULTS FOR PREDICTING POPULATION EMPLOYED.

Metric	Year	w/o DTKGCN	w/o GS	w/o LSTM	ECO-GROW
RMSE $\downarrow$	2019	11.474	11.977	12.092	<b>11.025</b>
	2020	14.809	31.886	14.651	<b>13.968</b>
	2021	14.607	17.866	14.410	<b>14.196</b>
	Average	13.630	20.576	13.718	<b>13.063</b>
MAE $\downarrow$	2019	5.440	5.436	5.485	<b>4.589</b>
	2020	6.557	9.970	6.212	<b>5.368</b>
	2021	7.246	8.073	6.920	<b>6.858</b>
	Average	6.414	7.826	6.206	<b>5.605</b>
$R^2\uparrow$	2019	0.959	0.960	0.959	<b>0.965</b>
	2020	0.932	0.840	0.932	<b>0.937</b>
	2021	0.940	0.928	0.939	<b>0.944</b>
	Average	0.944	0.910	0.943	<b>0.949</b>

a decrease in RMSE and MAE. However, when  $\lambda$  exceeds 0.5, performance begins to deteriorate. This pattern shows that the model leverages both the node classification task (which focuses on individual city growth patterns) and the link prediction task (which models the inter-city dependencies) effectively.

Similarly, for the sensitivity analysis for embedding size, we fix  $\lambda = 0.5$ . The results, shown in Figure 4 (b), indicate that an embedding size of  $d = 16$  achieves the best performance, balancing the model's ability to represent features with its complexity, while larger embedding sizes lead to overfitting and reduced generalization.

## VI. CONCLUSION

This paper introduces ECO-GROW, a multi-graph framework designed to model and predict urban economic vitality

### D. Parameters Sensitivity (RQ3)

We evaluate the sensitivity of the model to two critical hyperparameters:  $\lambda$ , which balances the node classification and link prediction tasks, and the embedding size  $d$ . In the sensitivity analysis for  $\lambda$ , we fix  $d = 16$ . In Figure 4 (a), we observe that, as  $\lambda$  increases from 0.1 to 0.5, there is

Metric	Year	w/o DTKGCN	w/o GS	w/o LSTM	ECO-GROW
RMSE $\downarrow$	2019	19816.097	26966.652	17269.829	<b>16029.035</b>
	2020	18804.240	16771.433	20732.783	<b>15303.907</b>
	2021	19317.750	20401.466	18571.407	<b>17710.724</b>
	Average	19312.696	21379.850	18858.007	<b>16347.888</b>
MAE $\downarrow$	2019	9315.993	11335.491	8781.204	<b>8199.070</b>
	2020	11244.288	10570.642	11465.346	<b>9439.828</b>
	2021	13630.000	13118.438	12718.232	<b>12332.495</b>
	Average	11396.760	11674.857	10988.261	<b>9990.464</b>
$R^2\uparrow$	2019	0.802	0.719	0.830	<b>0.855</b>
	2020	0.854	0.896	0.861	<b>0.909</b>
	2021	0.889	0.878	0.896	<b>0.905</b>
	Average	0.848	0.831	0.862	<b>0.889</b>

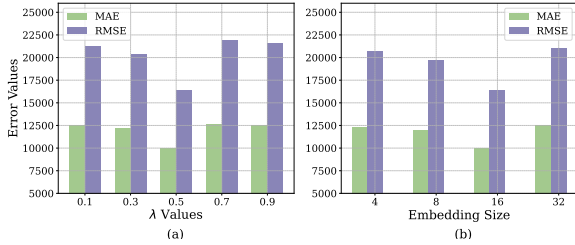


Fig. 4. Sensitivity Analysis of the parameters  $\lambda$  and  $d$  in predicting the number of new companies respectively.

across Chinese cities. By integrating industrial, regional, and mobility similarities, as well as temporal dynamics, ECO-GROW effectively captures the complex relationships driving urban economic development.

A key innovation of ECO-GROW is its use of complex prior knowledge to guide graph representation learning. Instead of directly predicting a value, our framework optimizes economic representations aligned with growth-related tasks, ensuring knowledge-rich and interpretable embeddings. The Graph Scorer adaptively learns the importance of static networks, while the DTKGCN dynamically selects the most relevant neighboring cities based on the characteristics of each graph type. These components enable ECO-GROW to generate accurate and robust representations.

This work demonstrates the model's capacity to enhance urban planning and policymaking by forecasting the key economic indicators, offering a tool to guide future urban growth strategies. Beyond predicting the number of new companies and employment population, the learned representations offer potential for broader applications, such as forecasting housing market trends or analyzing urban economic patterns. By open-sourcing our code, we aim to promote further research and practical applications in urban planning and sustainable development.

#### ACKNOWLEDGEMENT

This project was supported by the Science and Technology Commission of Shanghai Municipality (No. 25692108200).

#### REFERENCES

- [1] R. Nugroho, I. E. Wina Rachmawan, P. K. Rafif, and Ferrizal, “Integrating demand hotspots and adjusted spatial indexing for urban taxi demand prediction,” in *2024 IEEE International Conference on Big Data (BigData)*, 2024, pp. 8786–8789.
- [2] L. Li and W. Kong, “Quantitative assessment of urban economic vitality,” *Scientific Journal of Economics and Management Research*, vol. 2, no. 11, pp. 122–128, 2020.
- [3] Q. Lv and Z. Wu, “Evaluation of economic vitality of beijing and analysis of influencing factors—based on entropy method and grey correlation analysis model,” *Open Journal of Social Sciences*, 2020.
- [4] M. Zhang, T. Li, Y. Li, and P. Hui, “Multi-view joint graph representation learning for urban region embedding,” in *Proceedings of the 29th International Joint Conference on Artificial Intelligence*. IJCAI, 2020, pp. 4431–4437.
- [5] S. Wu, X. Yan, X. Fan, S. Pan, S. Zhu, C. Zheng, M. Cheng, and C. Wang, “Multi-graph fusion networks for urban region embedding,” in *Proceedings of the 31st International Joint Conference on Artificial Intelligence*. IJCAI, 2022.
- [6] S. Zhou, D. He, L. Chen, S. Shang, and P. Han, “Heterogeneous region embedding with prompt learning,” in *Proceedings of the AAAI Conference on Artificial Intelligence*, vol. 37, no. 4, 2023, pp. 4981–4989.
- [7] D. B. Audretsch and M. P. Feldman, “R&d spillovers and the geography of innovation and production,” *The American economic review*, vol. 86, no. 3, pp. 630–640, 1996.
- [8] J. Li, S. Chen, G. Wan, and C. Fu, “Spatial correlation and its interpretation of regional economic growth in china: Based on network analysis methods,” *Economic Research Journal*, vol. 49, no. 11, pp. 4–16, 2014.
- [9] T. N. Kipf and M. Welling, “Variational graph auto-encoders,” *NIPS Workshop on Bayesian Deep Learning*, 2016.
- [10] C. A. Hidalgo, B. Klinger, A.-L. Barabási, and R. Hausmann, “The product space conditions the development of nations,” *Science*, vol. 317, no. 5837, pp. 482–487, 2007. [Online]. Available: <https://www.science.org/doi/abs/10.1126/science.1144581>
- [11] D. Audretsch and M. Keilbach, “Entrepreneurship capital and economic performance,” *Regional studies*, vol. 38, no. 8, pp. 949–959, 2004.
- [12] Z. Acs, “How is entrepreneurship good for economic growth?” *Innovations: Technology, Governance, Globalization*, vol. 1, no. 1, pp. 97–107, 2006. [Online]. Available: <https://EconPapers.repec.org/RePEc:tpr:inntgg:v:1:y:2006:i:1:p:97-107>
- [13] J. Cheng, “Source of urban vitality: Systematic effects of migrant population on the development of urban economy,” *Chinese Journal of Urban and Environmental Studies*, 2019.
- [14] C. Xia, A. Zhang, and A. Yeh, “The varying relationships between multidimensional urban form and urban vitality in chinese megacities: Insights from a comparative analysis,” *Annals of the American Association of Geographers*, vol. 112, pp. 141 – 166, 2021.
- [15] B. Zhu and T. Zhang, “The impact of cross-region industrial structure optimization on economy, carbon emissions and energy consumption: A case of the yangtze river delta.” *The Science of the total environment*, vol. 778, p. 146089, 2021.
- [16] A. Grover and J. Leskovec, “node2vec: Scalable feature learning for networks,” in *Proceedings of the 22nd ACM SIGKDD International Conference on Knowledge Discovery and Data Mining*, 2016, pp. 855–864.
- [17] T. N. Kipf and M. Welling, “Semi-supervised classification with graph convolutional networks,” *CoRR*, vol. abs/1609.02907, 2016. [Online]. Available: <http://arxiv.org/abs/1609.02907>
- [18] P. Veličković, G. Cucurull, A. Casanova, A. Romero, P. Liò, and Y. Bengio, “Graph attention networks,” in *International Conference on Learning Representations*, 2018. [Online]. Available: <https://openreview.net/forum?id=rXJMpkCZ>
- [19] Z. Yao, Y. Fu, B. Liu, W. Hu, and H. Xiong, “Representing urban functions through zone embedding with human mobility patterns,” in *Proceedings of the 27th International Joint Conference on Artificial Intelligence*. IJCAI, 2018.
- [20] Y. Xi, Y. Liu, Z. Liu, S. Tarkoma, P. Hui, and Y. Li, “From pixels to progress: generating road network from satellite imagery for socioeconomic insights in impoverished areas,” in *Proceedings of the 33th International Joint Conference on Artificial Intelligence*, ser. IJCAI, 2024. [Online]. Available: <https://doi.org/10.24963/ijcai.2024/831>
- [21] X. Yong and X. Zhou, “Musecl: predicting urban socioeconomic indicators via multi-semantic contrastive learning,” in *Proceedings of the 33th International Joint Conference on Artificial Intelligence*, ser. IJCAI, 2024. [Online]. Available: <https://doi.org/10.24963/ijcai.2024/834>
- [22] Z. Xu and X. Zhou, “Cgap: urban region representation learning with coarsened graph attention pooling,” in *Proceedings of the 33th International Joint Conference on Artificial Intelligence*, ser. IJCAI, 2024. [Online]. Available: <https://doi.org/10.24963/ijcai.2024/832>
- [23] H. Peng, R. Zhang, Y. Dou, R. Yang, J. Zhang, and P. S. Yu, “Reinforced neighborhood selection guided multi-relational graph neural networks,” *ACM Transactions on Information Systems (TOIS)*, vol. 40, pp. 1 – 46, 2021.
- [24] S. Stetsenko and A. Moholivets, “Methodical approaches to forecasting and early detection of economic cyclicity,” *Ways to Improve Construction Efficiency*, 2021.
- [25] F. A. Gers, J. Schmidhuber, and F. Cummins, “Learning to forget: Continual prediction with lstm,” *Neural Computation*, vol. 12, pp. 2451–2471, 2000.
- [26] R. Tibshirani, “Regression shrinkage and selection via the lasso,” *Journal of the royal statistical society series b-methodological*, vol. 58, pp. 267–288, 1996. [Online]. Available: <https://api.semanticscholar.org/CorpusID:16162039>